GENERALIZED HARDI INVARIANTS BY METHOD OF TENSOR CONTRACTION

Yaniv Gur and Chris R. Johnson

SCI Institute, 72 S. Central Campus Dr., University of Utah, Salt Lake City, UT 84112, USA

ABSTRACT

We propose a 3D object recognition technique to construct rotation invariant feature vectors for high angular resolution diffusion imaging (HARDI). This method uses the spherical harmonics (SH) expansion and is based on generating rank-1 contravariant tensors using the SH coefficients, and contracting them with covariant tensors to obtain invariants. The proposed technique enables the systematic construction of invariants for SH expansions of any order using simple mathematical operations. In addition, it allows construction of a large set of invariants, even for low order expansions, thus providing rich feature vectors for image analysis tasks such as classification and segmentation. In this paper, we use this technique to construct feature vectors for eighth-order fiber orientation distributions (FODs) reconstructed using constrained spherical deconvolution (CSD). Using simulated and in vivo brain data, we show that these invariants are robust to noise, enable voxel-wise classification, and capture meaningful information on the underlying white matter structure.

Index Terms— Diffusion MRI, HARDI, invariants

1. INTRODUCTION

Invariants play an important role in diffusion MRI (dMRI). They represent tissue properties, such as diffusion anisotropy, and are used for registration, tissue segmentation and classification, as well as white matter integrity measures in clinical studies of debilitating brain diseases. Importantly, these features need to be rotation invariant to capture orientation independent tissue properties, as well as to enable comparisons across images that are not completely aligned. Modelling diffusion using second-order tensors, as in DTI, enable construction of diverse anatomically meaningful scalars, such as fractional anisotropy (FA), mean diffusivity (MD), and relative anisotropy (RA), which capture tissue microstructure, and are used to indicate anatomical changes [1]. Most of these scalars are derived using the tensor eigenvalues, hence, they are naturally rotation invariant as the eigenvalues remain intact under rotation. In HARDI, however, the situation is more complicated as the diffusion profile is described by higher-order tensors or orientation distribution functions (ODFs), and there is no straightforward generalization of DTI invariants to these models. The generalized FA (GFA), for example, aims to represent anisotropy in HARDI models, but has limited classification power, and is sensitive to noise being directly computed from a discrete representation of orientation distribution function (ODF) [2].

In order to take advantage of the enhanced modelling capabilities of HARDI compared to DTI, it is important to derive new invariants that capture tissue properties, and can be used as white matter biomarkers. Over the last years, researchers have created new invariants for HARDI-based models, for example, the generalized anisotropy (GA) and scaled anisotropy (SE) [3], as well as several approaches that are based on second and fourth-order tensor representations [4, 5]. A recent approach uses the Gaunt coefficients to construct invariants for ODFs and HARDI signals using the more general SH representation [2].

Our proposed technique follows a similar path of using the SH representation. We then leverage the idea of invariants constructed by tensor contraction used in computer vision for 3D pattern recognition [6]. The original idea emerged from the theory of angular momentum addition in quantum physics, and although it relies on deep and complex theoretical foundations, the formulation enables systematic construction of invariants in an elegant and simple way. This method is general, as it enables extraction of invariants from any 3D object represented as a SH series. Therefore, it can be used to construct invariants from the dMRI signal, or from any diffusion modelling object, such as ODF or FOD. In addition, it enables direct construction of invariants for any expansion order, thus, it is not limited to the common second or fourth order expansions. This method generalizes the SH descriptors used in [7] to classify autism spectrum disorder (ASD) patients and controls, and to segment brain tissue [8, 9]. It is based on constructing contravariant rank-1 tensors (vectors) using the SH and Clebsch-Gordan (CG) coefficients, and contracting them with covariant vectors to obtain rank-0 tensors (invariants). This process can be continued repeatedly to build as many invariants as desired regardless of the SH order, therefore, enables the construction of long feature vectors with strong classification capabilities. This is an advantage over the method presented in [2] in which the maximal number of invariants is bounded by the rank of the Toeplitz-like matrix.

This work was funded in part by the NIH/NCRR Center for Integrative Biomedical Computing, P41RR12553.

978-1-4673-1961-4/14/$31.00 ©2014 IEEE

We demonstrate the strengths of our approach in both synthetic and in vivo experiments. Using simulated data we show that these invariants are robust to noise and can classify voxels based on the number of fiber compartments and their diffusivities. Using in vivo brain data, we show that they capture anatomically meaningful information, and may be used as white matter integrity measures.

2. CONSTRUCTION OF INVARIANTS

Given a basis $\{e_i\}$, one can write a vector in this basis using the expansion coefficients, such that $\mathbf{v} = c^i e_i$. The expansion coefficients are components of a contravariant rank-1 tensor (vector), and are denoted with upper indices. On the other hand, the elements of a covariant vector (dual vector) are denoted with lower indices: $\mathbf{v} = c_i e^i$. When $\{e_i\}$ is an orthonormal basis as in our case, contravariant and covariant vectors are simply complex conjugates of each other. The tensor contraction operation multiplies a contravariant with a covariant tensor, such that repeated lower and upper indices are summed in the Einstein summation convention. This operation is equivalent to an inner product, thus, a contraction of two vectors yields a scalar (an invariant): $s = c^i c_i$.

Let f be a continuous spherical function. According to Fourier's theorem on the sphere, it can be expanded in a spherical harmonics (SH) basis, such that

$$f(\theta, \phi) = \sum_{l=0}^{\infty} \sum_{m=-l}^{l} c_l^m Y_l^m, \tag{1}$$

where the Y_l^m denotes the SH, and the c_l^m's are complex expansion coefficients. In practice, when representing 3D objects, the infinite sum is truncated at a finite order L. In our case, the function f may represent the dMRI signal given at a discrete set of gradient directions, an orientation distribution function (ODF), a fiber orientation distribution (FOD), or even a higher-order tensor representation of the diffusion profile using the appropriate coefficients transformation. Thus, this representation is not restricted to a particular reconstruction technique. While in general there is no restriction on L, most HARDI reconstruction techniques are based on even order expansions.

While the common HARDI reconstruction technique uses the real SH expansion, the method described here is based on the complex SH representation. Therefore, the real coefficients computed by the various reconstruction algorithms are transformed to the complex domain using the following relation:

$$c_l^m = \begin{cases} \frac{1}{\sqrt{2}}(\hat{c}_{lm} + i\hat{c}_{l\,-m}) & \text{if } m > 0 \\ \hat{c}_{l0} & \text{if } m = 0 \\ (-1)^m(\hat{c}_l^{-m})^* & \text{if } m < 0, \end{cases} \tag{2}$$

where $\hat{c}_{lm}$ denotes the real coefficients, and $*$ stands for the complex conjugate.

The SH form an orthonormal basis of the Hilbert space of square-integrable functions. An important observation is that this space can be decomposed into a set of subspaces, each associated with a specific l value and is spanned by the spherical harmonics $Y_l^m, \quad -l \leq m \leq l$. We will denote these subspaces using the subscript l as V_l, that is, $V_l = \mathrm{Span}\{Y_l^{-l}, Y_l^{-l+1}, \ldots, Y_l^{l-1}, Y_l^l\}$. These subspaces correspond to irreducible representations of the rotation group, $SO(3)$. Thus, each of these subspaces is globally rotational invariant, that is, given a vector $f \in V_l$ and a rotation R, we have $R(f) \in V_l$. This property enables us to construct rotation invariants by contracting contravariant and covariant vectors defined in V_l.

The first set of invariants are constructed by contracting the SH coefficients, c_l^m, for a given l. Being expansion coefficients, they are contravariant components of a vector in V_l. Therefore, by contracting them with their covariant counterparts, we construct a tensor of order zero (a scalar), which is rotation invariant:

$$I_l = c_l^m c_{lm} = \sum_{m=-l}^{l} c_l^m (c_l^m)^*. \tag{3}$$

These set of invariants are the well-known power spectrum SH descriptors used in various biomedical applications as an input to the SVM classifier [7, 9], as well as in 3D object recognition in computer vision [10]. Despite their usefulness, as we show here, these invariants are sensitive to noise and may lead to misclassification of objects. For example, ODFs describing similar white matter structure may be classified into separate groups due to the impact of noise. Since the SNR in HARDI scans is generally low, robustness to noise is an important property. In addition, given the maximal ODF order L, only $L/2 + 1$ such invariants exist (for even L values), resulting in limited classification power. However, it turns out that these invariants are a particular case of a richer set of invariants that are constructed by mixing tensors from different subspaces, and contracting them. This idea originated from the theory of angular momentum addition in two-particle systems in quantum mechanics [11]. It also corresponds to decomposing reducible representations of the rotation group, $SO(3)$, into irreducible ones. The main elements here are the CG coefficients (known also as the Wigner coefficients), which are used to couple the subspaces. Using these coefficients, one can construct new contravariant rank-1 tensors in V_l as follows:

$$\begin{aligned} T_{l,l_1,l_2}^m &= k_{l,l_1,l_2}^{m,m_1,m_2} c_{l_1 m_1} c_{l_2 m_2} \\ &= \sum_{m_1=-l_1}^{l_1} \sum_{m_2=-l_2}^{l_2} k_{l,l_1,l_2}^{m,m_1,m_2} (c_{l_1}^{m_1})^* (c_{l_2}^{m_2})^*, \end{aligned} \tag{4}$$

where $k_{l,l_1,l_2}^{m,m_1,m_2}$ are the CG coefficients. The computed tensors can be contracted with the SH coefficients to create a new

set of invariants:

$$J_{l,l_1,l_2} = T^m_{l,l_1,l_2} c_{lm} = \sum_{m=-l}^{l} T^m_{l,l_1,l_2} (c^m_l)^*. \quad (5)$$

In addition, they can be contracted with each other to build another set of invariants:

$$K_{l,l_1,l_2,l_3,l_4} = T^m_{l,l_1,l_2} T_{l,l_3,l_4,m} = \sum_{m=-l}^{l} T^m_{l,l_1,l_2} (T^m_{l,l_3,l_4})^*. \quad (6)$$

As shown here, the computation of these invariants only involves multiplications of coefficients and a summation. The CG coefficients are available in tables, and can also be computed using recurrence relations.

The process of constructing tensors in V_l and contracting them can be continued as desired to produce more invariants. For example, one can use the tensors T^m_l to generate new tensors in V_l, and then contract them with the SH coefficients, the T^m_l's, or with themselves. However, the three sets of invariants I, J and K already provide long feature vectors, even for low expansion orders (e.g., $L = 2$). Finally, the conditions under which these invariants can be computed are $|l_1 - l_2| \leq l \leq (l_1 + l_2)$ for J, and the additional condition $|l_3 - l_4| \leq l \leq (l_3 + l_4)$ for K, whereas the I invariants can be computed for any l ($l = 0, 2, \ldots, L$). Further symmetry relations can be used to reduce the number of invariant, however, we will not consider this aspect in this short paper.

3. RESULTS

3.1. Synthetic data

In this experiment, we simulated the signal using the multi-tensor model with diffusivities [1.7e-3, 3e-4, 3e-4] for each tensor. The signal was corrupted by Rician noise with a baseline SNR of 20. We generated 100 repetitions of randomly rotated ODFs for each of the following cases: one fiber, two fibers crossing at 60 degrees with equal mixing weights, and three fibers with equal mixing weights (the two fibers case with a third orthogonal fiber). For each ODF we computed 10 different invariants: I_l, $l = 0, 2, \ldots, 8$ and $J_{0,2,2}$, $J_{2,2,2}$, $J_{4,2,2}$, $J_{6,4,4}$, $J_{8,4,4}$. Then, we plotted the first three invariants as vectors in $\mathbb{R}^3$ for both the I and J invariants (Fig. 1). We used the variances computed using PCA to measure the concentration of the point clouds in $\mathbb{R}^5$ generated by these invariants. Fig. 1 and Table 1 show that both sets of invariants could classify the different fiber configurations into three distinct groups corresponding to voxels with one, two, or three fibers. However, these results also show that the J invariants are more robust to noise as their associated point clouds are more compact.

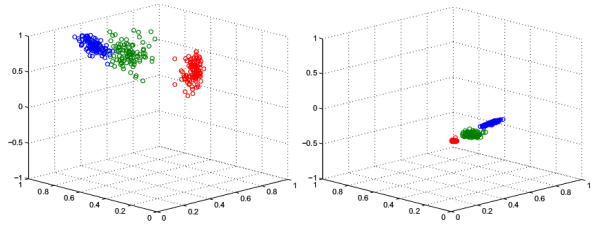

Fig. 1. Number of fiber classification using the I invariants (left), and the J invariants (right). The point clouds correspond to one fiber (blue), two fibers (green), and three fibers (red).

		Variance				
1F	I	0.0336	0.0176	0.0065	0.0040	0.0013
	J	0.0190	0.0063	0.0011	0.0008	0.0008
2F	I	0.0246	0.0193	0.0153	0.0049	0.0040
	J	0.0063	0.0038	0.0034	0.0019	0.0007
3F	I	0.0263	0.0125	0.0074	0.0052	0.0035
	J	0.0040	0.0030	0.0011	0.0010	0.0007

Table 1. Variance comparisons using PCA. The labels 1F, 2F and 3F correspond to one, two, or three fibers, respectively. The labels I and J indicate the invariant type, and each row presents the vector of invariants beginning with $l = 0$ (left).

3.2. Simulated phantom

In this experiment, we extracted the invariants $J_{0,2,2}$, $J_{2,2,2}$, and $J_{4,2,2}$ from 8th-order FODs reconstructed from a slice of the 3D simulated phantom used for comparisons at the HARDI reconstruction ISBI challenge [12]. This phantom is composed of voxels containing fiber configurations differing by the number of compartments, and the compartment diffusivities used to simulate the signal. To compute the invariants we used the phantom simulated at SNR=30. After computing the set of 3 invariants for each FOD, we plotted them as vectors in RGB space. The results presented in Fig. 2 show that using these invariants as feature vectors we were able to classify the voxels not only based on the number of fibers, but also based on differences in compartment diffusivities. The previously discussed robustness to noise of the J invariants compared to the I invariants is clearly shown.

3.3. In vivo brain data

The brain data was acquired on a 3T Siemens Alegra machine using 60 diffusion weighted directions, 10 baseline scans, and a b-value of 2000. For the voxels within the brain mask, we reconstructed 8th-order FODs using CSD, and computed a set of J invariants. In addition, we computed the GFA map for comparison. The results, presented in Fig. 3, show that these invariants describe white matter structures, such as the corpus callosum, and the superior and inferior longitudinal fasci-

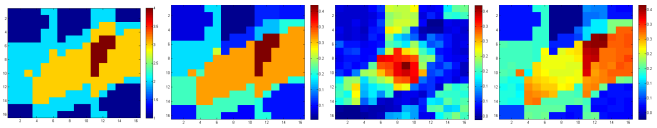

Fig. 2. Voxel-wise classification of the simulated ISBI'12 challenge phantom. From left to right: the ground-truth number of fibers map, the same map segmented according to the principal diffusivities, voxel-wise classification using the I invariants, and the J invariants.

culi (ILF and SLF). Interestingly, these results also show that these invariants describe anisotropy by high intensity values, for example, in the corpus callosum area. Thus, in addition to their classification abilities, these invariants can be used as rotation invariant integrity measures and may indicate structural changes in white matter. For comparison, the GFA map (bottom right) appears to be noisy and presents white matter structures less clearly. It is also shown that the invariant corresponding to the 6th-order show less structure and captures mostly noise. This may indicate that the data is very noisy, but it also raises a question whether higher-order invariants can be used for denoising or for extracting features from a noisy background.

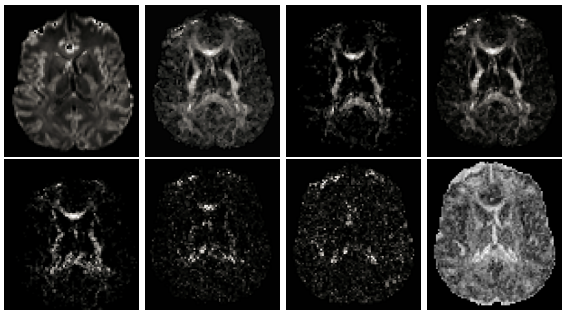

Fig. 3. Maps of the J invariants extracted from in vivo brain data. Top (L to R): $J_{0,0,0}$, $J_{0,2,2}$, $J_{2,2,2}$, and $J_{2,2,0}$. Bottom: $J_{4,2,2}$, $J_{4,4,2}$, $J_{6,4,4}$, and GFA.

4. CONCLUSIONS

In this paper, we applied tensor contraction techniques used in 3D object recognition to generate invariants for HARDI models. This technique allows us to compute invariants for the dMRI signal, or any HARDI reconstruction model that uses SH expansion. It provides a systematic procedure to construct invariants for any given SH truncation order using simple operations, and it can generate as many invariants as desired, regardless of the expansion order. We used simulated and in vivo brain data to show that these invariants are robust to noise, enable voxel-wise classification, and capture white matter structure.

5. REFERENCES

[1] Denis Le Bihan, Jean-Franois Mangin, Cyril Poupon, Chris A. Clark, Sabina Pappata, Nicolas Molko, and Hughes Chabriat, "Diffusion tensor imaging: Concepts and applications," *Journal of Magnetic Resonance Imaging*, vol. 13, no. 4, pp. 534–546, 2001.

[2] Evan Schwab, H. Ertan etingl, Bijan Afsari, Michael A. Yassa, and René Vidal, "Rotation invariant features for HARDI," in *Information Processing in Medical Imaging*, vol. 7917 of *LNCS*, pp. 705–717. 2013.

[3] Evren Özarslan, Baba C. Vemuri, and Thomas H. Mareci, "Generalized scalar measures for diffusion MRI using trace, variance and entropy," *Magn. Reson. Med.*, vol. 53, pp. 866–876, 2005.

[4] A. Fuster, J. van de Sande, L.J. Astola, C. Poupon, J. Velterop, and B.M. ter Haar Romenij, "Fourth-order tensor invariants in high angular resolution diffusion imaging," in *Computational Diffusion MRI Workshop (CDMRI), MICCAI*, Toronto, Canada, 2011.

[5] Aurobrata Ghosh, Théodore Papadopoulo, and Rachid Deriche, "Biomarkers for HARDI: 2nd & 4th order tensor invariants," in *IEEE International Symposium on Biomedical Imaging*, Barcelona, Spain, May 2012.

[6] Gilles Burel and Hugues Hnocq, "Three-dimensional invariants and their application to object recognition," *Signal Processing*, vol. 45, no. 1, pp. 1 – 22, 1995.

[7] Luke Bloy, Madhura Ingalhalikar, Harini Eavani, TimothyP.L. Roberts, Robert T. Schultz, and Ragini Verma, "HARDI based pattern classifiers for the identification of white matter pathologies," in *MICCAI 2011*, vol. 6892 of *LNCS*, pp. 234–241. 2011.

[8] Lawrence R. Frank, "Characterization of anisotropy in high angular resolution diffusion-weighted MRI," *Magn. Reson. Med*, vol. 47, pp. 1083–1099, 2002.

[9] Henrik Skibbe and Marco Reisert, "Rotation covariant image processing for biomedical applications," *Computational and Mathematical Methods in Medicine*, pp. 908–915, 2013.

[10] Michael Kazhdan, Thomas Funkhouser, and Szymon Rusinkiewicz, "Rotation invariant spherical harmonic representation of 3D shape descriptors," in *Proceedings of Eurographics*, 2003, SGP '03, pp. 156–164.

[11] C. Cohen-Tannoudji, B. Diu, and F. Laloë, *Quantum mechanics, Vol 2*, Wiley, 1977.

[12] "HARDI reconstruction challenge," `http://hardi.epfl.ch/static/events/2012_ISBI/`, Barcelona, Spain, 2012.